Journal of Photochemistry and Photobiology A: Chemistry 214 (2010) 100–107

Contents lists available at ScienceDirect

Journal of Photochemistry and Photobiology A: Chemistry

journal homepage: www.elsevier.com/locate/jphotochem

Excited state double proton transfer of a 1:1 7-azaindole:H_2O complex and the breakdown of the rule of the geometric mean: Variational transition state theory studies including multidimensional tunneling

My Phu Thi Duong, Kisoo Park, Yongho Kim*

Department of Applied Chemistry, Kyung Hee University, 1 Seochon-dong, Giheung-gu, Yongin-si, Gyeonggi-do 446-701, Republic of Korea

ARTICLE INFO

Article history:
Received 19 February 2010
Received in revised form 16 May 2010
Accepted 16 June 2010
Available online 23 June 2010

Keywords:
Excited state double proton transfer
7-Azaindole–water complex
Rule of geometric mean
Concerted albeit asynchronous mechanism
Kinetic isotope effects
Variational effect

ABSTRACT

The rule of the geometric mean in rates and kinetic isotope effects has long been used as a criterion for identifying the reaction mechanism, e.g., stepwise vs. concerted, for double proton transfer reactions. Potential energy surfaces of double proton transfers for excited state tautomerization in a 1:1 7-azaindole:H_2O complex were generated at the MRPT2//CASSCF(10,9)/6-31G(d,p) level. Variational transition state theory, including multidimensional tunneling approximation, was used to calculate rates and kinetic isotope effects. No intermediates were present along the reaction coordinate. Two protons in the excited state tautomerization were transferred concertedly, albeit asynchronously. Positions of the variational transition states depend very much on the isotopic substitution. The asynchronicity of two protons in flight breaks the underlying assumption of the rule of the geometric mean so that the relation, $k_{HH}/k_{HD} \approx k_{HD}/k_{DD}$, is no longer valid in the excited state double proton transfer. Breakdown of the geometric mean rule does not necessarily entail that the reaction mechanism is stepwise; therefore this rule should be used very carefully as a criterion for identification of the mechanism.

1. Introduction

Proton transfer is one of the simplest and the most fundamental reactions in chemistry, and such as has been studied extensively [1,2]. The majority of studies have been done on single proton transfer, and multi-proton transfers have not been studied as extensively. The dynamics of multi-proton transfer is more complicated than that of a single proton transfer, and the detailed underlying mechanisms are not yet fully understood. One of the fundamental questions when studying double proton transfer reactions is their mechanism: concerted vs. stepwise. Examples of multi-proton transfer include proton relay systems in enzymes, proton transfer in hydrogen-bonded water complexes, and prototropic tautomerisms in nucleic-acid base pairs. Limbach et al. [3,4] studied double proton transfer in prototropic tautomerisms across many hydrogen-bonded systems and porphyrins using the dynamic NMR technique. They reported rates and kinetic isotope effects for both concerted [5] and stepwise [6,7] double proton transfer reactions. Tautomerization through bridging hydrogen bonds in a 7-azaindole (7AI) system is an interesting model for biological systems that has been extensively studied experimentally and theoretically [8–15]. Although tautomerization in the 7AI complex is one of the most extensively studied reactions, the mechanism of the excited state double proton transfer (ESDPT) has not been fully resolved [9,15–17]. The 7AI molecule has an N–H bond and a heteroaromatic N atom as hydrogen bond donor and acceptor sites, respectively, and the normal form becomes unstable with respect to the tautomer form in the S_1 state [18,19].

The excited state tautomerization in 7AI has been observed in the condensed phase in alcohol or water solutions [10,20,21]. The tautomerization of 7AI in alcohols has been discussed in terms of a two-step process [22–24]. The first step involves solvent reorganization to form a cyclically hydrogen-bonded 7AI–alcohol complex, while the second step is an intrinsic double proton transfer.

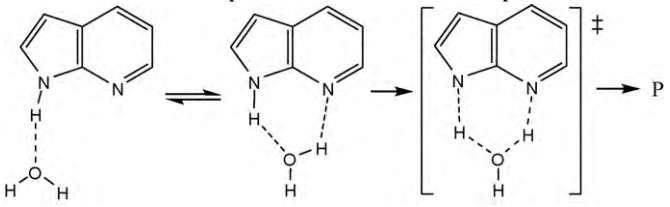

If the solvent motion was rate limiting, no significant kinetic isotope effect (KIE) would be expected. However, KIEs for excited state tautomerization have been observed in 7AI complexes with various alcohols [10,22,24], and Moog and Maroncelli [24] suggested that both solvent reorganization and the intrinsic proton trans-

* Corresponding author. Tel.: +82 31 201 2456; fax: +82 31 203 5773.
E-mail address: yhkim@khu.ac.kr (Y. Kim).

1010-6030/$ – see front matter © 2010 Elsevier B.V. All rights reserved.
doi:10.1016/j.jphotochem.2010.06.015

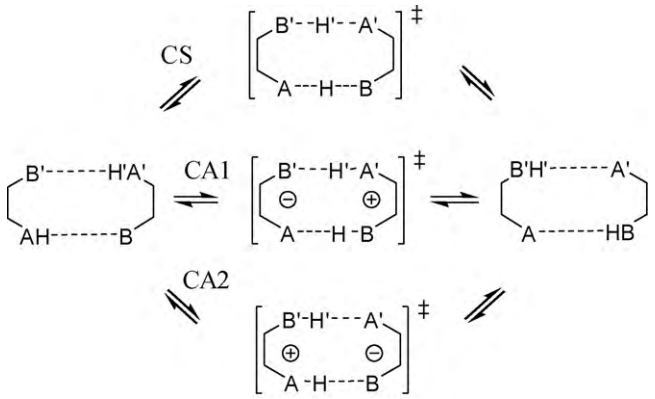

Scheme 1. Concerted synchronous (CS) and asynchronous (CA) double proton transfer processes.

fer step determined the reaction rate. Chen et al. [10] suggested that two protons were transferred concertedly in the intrinsic double proton transfer step based on the observed rates and KIEs satisfying the rule of geometric mean (RGM). Chou et al. [25] measured rates and KIEs for ESDPT of a 1:1 3-cyano-7AI:water complex to clarify the mechanism of 7AI in water. These authors and others [20,23,25,26] suggested that a fast, excited state equilibrium between the 1:1 cyclic hydrogen-bonded complex and randomly hydrated complexes was established and followed by ESDPT that may be governed by a tunneling mechanism. However, the mechanism of ESDPT in water remains unclear. Chen et al. [10] observed the breakdown of the RGM in water and suggested the stepwise ESDPT mechanism. The observed HH/DD KIEs in water were in the range of 3.4–3.9 at room temperature [10,20,25], and these small KIE values might also be supportive for a stepwise mechanism. Evidence of concerted vs. stepwise pathways for double proton transfer reactions with meta-stable intermediate is often manifested through the proton inventory and the RGM, where $k_{HD} = (k_{HH}k_{DD})^{1/2}$, i.e. $k_{HH}/k_{HD} \approx k_{HD}/k_{DD}$ for KIEs [5,10,27–31]. However the most well known breakdown of the RGM for a concerted multi-proton transfer is due to tunneling [5,30–33], and many theoretical studies suggested a concerted mechanism for ESDPT in 1:1 7AI:H_2O complexes. In early theoretical calculations, Chaban and co-workers [18,19] investigated the ground and excited state tautomerization process in 7AI with and without mediating solvent using *ab initio* calculations and showed that the ESDPT in the 7AI:H_2O complex occurred via a concerted process. Very recently, Kina et al. [34] utilized *ab initio* molecular dynamics (AIMD) simulations for the 7AI:H_2O complex which showed that ESDPT occurs concertedly, albeit asynchronously, both in the gas phase and in solution.

The breakdown of the RGM has long been used as an evidence of stepwise mechanism for double proton transfer reactions with meta-stable intermediate. The underlying assumptions of the RGM are that (1) the changes in force constants of isotopically sensitive bonds at the transition state that are broken or formed during the concerted reaction are approximately the same, and (2) the secondary KIE is negligible. In general, the first assumption is applicable when the two reactive sites are chemically equivalent, and bond breaking and formation occur synchronously. The second assumption is only applicable if the two reactive sites are chemically independent. In some cases, however, the RGM breaks down due to violation of the basic assumption that the force constant changes at the transition state are not the same among the isotopically sensitive bonds. One can consider several different types of concerted multi-proton transfer processes as shown in Scheme 1. In a concerted synchronous (CS) double proton transfer, the breaking of A–H and A′–H′ bonds occurs in unison, along with the bond forming of B–H and B′–H′. In this process, the sum of the A–H and H–B bond order is not necessarily conserved. If the A and A′ and B and B′ atoms are the same, the transition state of the CS process will have C_2 or approximately C_2 symmetry, at least locally. In a concerted asynchronous (CA) process, the breaking of A–H and A′–H′ bonds and the formation of B–H and B′–H′ bonds do not occur in unison. At the transition state of the CA1 process, bond breaking of A–H is nearly complete while the bond breaking of A′–H′ has hardly begun. However, B′–H′ bond formation is also nearly complete, but the B–H bond is not yet formed. The transition state of this process would have an ion-pair character. The CA2 process is the same as the CA1 process with the exception of the bond breaking and bond making order. When the A, A′, B, and B′ atoms are all the same, the transition state will show approximately C_{2v} symmetry.

In general, when the reaction moves from reactants to the transition state, the change in force constants of A···H···B and A′···H′···B′ are approximately the same for the CS process, but not for the CA processes. As a result, it is clear that the RGM will generally work for the CS process, but not when the process is asynchronous. In an extreme case where the change in force constants of A–H and A′–H′ are very different (when two reactive sites are not chemically equivalent), the RGM may not necessarily hold, even for the CS process. In contrast, if the net changes in force constants for A···H–B and A′–H′···B′ are approximately the same as in the CA1 process (as shown in the TS of the formamidine dimer in a polar solution) [35], the RGM will be valid even when the bond breaking and bond making processes are not synchronized. Therefore, the RGM will work in a special concerted process where the changes in force constants for the two reactive sites are approximately the same, regardless of their synchronicity. Asynchronous multi-proton transfers have been reported previously [34–40]. The breakdown of the RGM has recently been reported in concerted and asynchronous double proton transfer reactions [38]. If the changes in the force constants are not the same and the multi-proton transfer is asynchronous, the RGM will not necessarily hold even for the concerted process. Therefore, the breakdown of the RGM may not be sufficient evidence for a stepwise mechanism.

The stepwise ESDPT mechanism of a 1:1 7AI:H_2O complex in water was suggested after experimental observations of the breakdown of the RGM [10]. Because asynchronicity and tunneling result in the breakdown of the RGM in the concerted double proton transfer, excited state reaction dynamics calculations would be required to understand these experimental results correctly in terms of the reaction mechanism. For this, both a multidimensional potential energy surface in the excited state and a dynamics theory that can handle multidimensional tunneling in large molecular systems is needed. In this study, multidimensional potential energy surfaces were generated using the interpolated variational transition state theory by mapping (IVTST-M) method [41] at the MRPT2//CASSCF(10,0)/6-31G(d,p) level of theory. We calculated vibrationally adiabatic energy surfaces in the S_1 electronic state of the ESDPT in isotopically substituted 7AI:H_2O complexes. These adiabatic energy surfaces were used to calculate rates and KIEs using variational transition state theory including multidimensional tunneling approximations. The computed KIEs were used to test the RGM and compared with experimental results. The breakdown of this rule will be discussed in terms of the reaction dynamics and the mechanism of the ESDPT.

2. Computational methods

Geometries of the reactant complex, product complex, and the transition state (TS) in the excited electronic state were optimized at the CASSCF(10,9)/6-31G(d,p) level using the GAUSSIAN03 quantum mechanical package [42]. Zero-point energies (ZPEs) were

calculated at the same level. Single point energy calculations were also carried out using the second order multireference perturbation theory (MRPT2) [43–45] for the stationary points. We performed polarizable continuum model calculations using the integral equation formalism (IEFPCM) [46–48] for cyclic and non-cyclic reactant complexes and TS to elucidate the mechanism of ESDPT in water. GAUSSIAN09 program [49] was used for the solvent effect calculations.

Reaction coordinates were obtained by calculating the minimum energy path (MEP) from TS to reactant and product. The MEP was initially obtained in the mass-scaled coordinate by 1 amu at the CASSCF(10,9)/6-31G(d,p) level. The interpolated variational transition state theory by mapping [41] (IVTST-M) algorithm was used to construct the potential and vibrationally adiabatic energy curves in the S_1 electronic state with 31 Hessian and 310 gradient points, which was denoted as IVTST-M-31/310. This potential energy curve was corrected by 31 interpolated single point energies (ISPE) [50] along the MEP with MRPT2 such that the interpolation could generate the needed points of high-level potential energy surfaces for the rate calculations. These non-stationary Hessian and high-level energy points were chosen every 0.1 bohr between −2.3 and 0.8 bohr along the MEP. Therefore the final potential energy curves along the MEP in this study were obtained at the dual-level, interpolated MRPT2//CASSCF(10,9)/6-31G(d,p). The vibrationally adiabatic energy in the S_1 electronic state was calculated as the sum of the ZPE and the potential energy, which were called "adiabatic energy" in this study. All MRPT2 calculations were performed using the GAMESS program [51]. Zero-point energies are very important to obtain accurate adiabatic energy curves. It was practically impossible to calculate vibration frequencies in the excited state using the MRPT2 method to consider the dynamic electronic correlation. Since the CASSCF method overestimates the N–H, O–H, and other frequencies, all Hessian used in this study were scaled to reduce CASSCF frequencies by a factor of 0.9.

Reaction rates were calculated using variational transition state theory [52–55], which included a multidimensional semiclassical tunneling approximation. The Born–Oppenheimer potential on the MEP was called $V_{MEP}(s)$, where s is the reaction coordinate parameter and the canonical variational transition state theory rate constant is given by:

$$k^{CVT}(T) = \min_{s} k^{GT}(T, s) = \sigma \frac{k_B T}{h} \frac{Q^{GT}(T, s_*^{CVT})}{\Phi^R} \exp[-\beta V_{MEP}(s_*^{CVT})]. \quad (1)$$

The superscript GT denotes the generalized transition state theory; β is $1/k_BT$; k_B is the Boltzmann constant; h is Planck's constant; s_*^{CVT} is the value of s at which k^{GT} is minimum, or the location of the canonical variational transition state (CVT); σ is the symmetry factor; and Q^{GT} and Φ^R are partition functions for the generalized transition state (GTS) and reactants, respectively.

To include the tunneling effect, the calculated rate constant $k^{CVT}(T)$ is multiplied by a transmission coefficient, κ^{SCT}

$$k^{CVT/SCT}(T) = k^{SCT}(T) k^{CVT}(T). \quad (2)$$

The transmission coefficient is defined as the ratio of the thermally averaged quantal ground-state transmission probability, $P(E)$, to the thermally averaged classical transmission probability for the effective potential along the reaction coordinate. When the reaction path curvature was small, tunneling was assumed to occur on a path defined by the classical turning points on the concave side of the MEP. This is an example of corner-cutting tunneling [52–54]. The centrifugal-dominant small-curvature semiclassical adiabatic ground state (CD-SCSAG) tunneling approximation was used to calculate $P(E)$. The CD-SCSAG method is referred to as "small-curvature tunneling" (SCT). All rate calculations were carried out by direct dynamics [56,57] with the IVTST-M [41] algorithm and interpolated single point energies (ISPE) along the MEP using the GAUSSRATE [58] program, which is an interface of GAUSSIAN [42] and the POLYRATE [59] dynamics program.

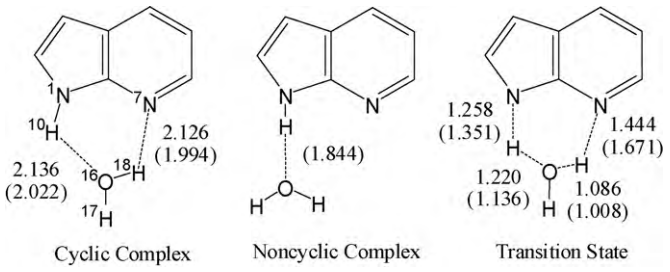

Fig. 1. Selected bond lengths in Å for the reactant, transition state, and product in the S_1 electronic state calculated at the CASSCF(10,9)/6-31G(d,p) level in the gas phase and in solution (numbers in parenthesis).

3. Results

The geometric parameters for the reactant, product, and the transition state (TS) in the excited state calculated at the CASSCF(10,9)/6-31G(d,p) level in the gas phase and aqueous solution are illustrated in Fig. 1. The non-cyclic 7AI:H_2O complex was not able to be obtained in the gas phase, because its energy is higher than the cyclic complex, so all calculations for geometry optimization resulted in the cyclic complex.

In the gas phase, the ^{16}O–^{18}H and ^{1}N–^{10}H distances at the conventional TS (saddle point) were 0.134 and 0.259 Å longer than those at the reactant, respectively. The ^{10}H moved more than halfway from ^{1}N toward ^{16}O atoms but the ^{18}H atom moved very little. Such asynchronous double proton transfer generated a H_3O^+-like moiety in part of the TS. The asynchronicity of the ESDPT became more significant in aqueous solution. The ^{16}O–^{18}H and ^{1}N–^{10}H bond distances in water were increased by 0.05 and 0.34 Å, respectively, as compared with those at the reactant, respectively. The formation of the H_3O^+-like moiety in part of the TS became more apparent in solution. This structure is very close to the possible intermediate of single proton transfer from ^{1}N to ^{16}O, which is an ion-pair with a H_3O^+-like moiety in it. However, no such intermediate was found. All computations for the intermediate went to either reactant or product.

Reaction energies and barrier heights for the intrinsic ESDPT at various levels of theory were listed in Table 1. The energy of the non-cyclically hydrogen-bonded 7AI:H_2O complex in water was about 1.92 kcal/mol higher than the cyclically hydrogen-bonded one. This

Table 1
Reaction energies and barrier heights for the double proton transfer in the excited state[a].

Computational method	ΔV (kcal/mol)	ΔE (kcal/mol)
CASSCF(10,9)/DZP(d,p)[b]	18.20 (14.7)	−31.80 (−31.2)
CASSCF(10,9)/6-31G(d,p)	18.08 (14.39)	−28.56 (−27.92)
IEFPCM/CASSCF(10,9)/6-31G(d,p)	16.64 [16.01][c]	−26.27
MCQDPT2//CASSCF(10,9)/DZP[d]	9.80 (6.3)	−18.00 (−17.4)
MRPT2//CASSCF(10,9)/6-31G(d,p)	9.72 (6.03)[d]	−18.95 (−18.31)[d]
MRPT2/6-311G(d,p)//CASSCF(10,9)/6-31G(d,p)	9.10 (5.41)[d]	

[a] The numbers in parentheses include zero-point energies.
[b] Ref. [18].
[c] Including non-electrostatic interactions.
[d] Zero-point energies at the CASSCF(10,9)/6-31G(d,p) level were used.

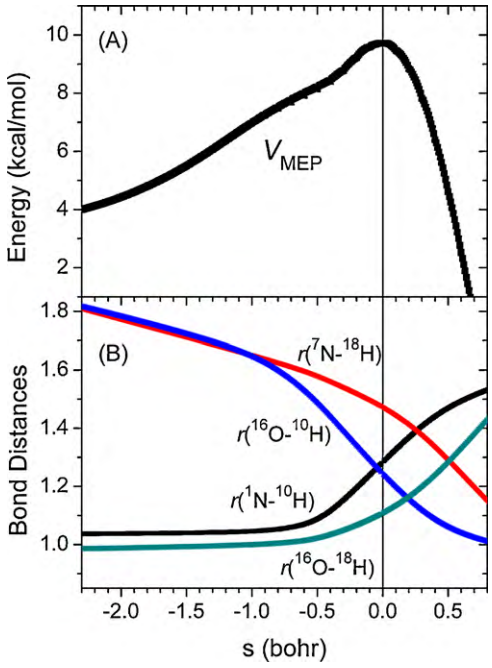

Fig. 2. (A) Potential energy curve and (B) selected bond distances in Å in the S_1 electronic state along the reaction coordinates of ESDPT in 1:1 7AI:H_2O complex calculated at the MRPT2//CASSCF(10,9)/6-31G(d,p) level. The vertical line represents the position of the conventional transition state.

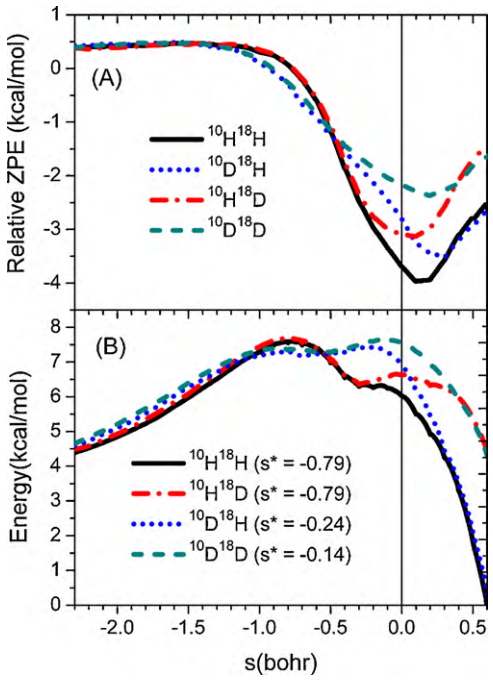

Fig. 3. (A) Relative zero-point energies in terms of corresponding reactant values and (B) vibrationally adiabatic energies in the S_1 electronic state along the reaction coordinates of the ESDPT for isotopically substituted 7AI:H_2O complexes calculated at the MRPT2//CASSCF(10,9)/6-31G(d,p) level. The vertical line represents the position of the conventional transition state, and the s^* values represent the maximum in the adiabatic energy curves.

result supports the suggestion that an excited state equilibrium between the 1:1 cyclic hydrogen-bonded complex and randomly hydrated complexes is established in water [20,23,25,26]. The MRPT2 barrier height of the ESDPT using the structures optimized at the CASSCF(10,9)/6-31G(d,p) level was 9.72 kcal/mol without ZPE corrections, which agreed very well with the corresponding MCQDPT2 values [18]. The use of the 6-311G(d,p) basis sets reduced this barrier slightly to 9.10 kcal/mol. The solvent effect reduced the CASSCF barrier again by about 2.07 and 1.44 kcal/mol with and without non-electrostatic interactions, respectively. Therefore the best estimate for the barrier height of the ESDPT in water would be about 7 kcal/mol without ZPE corrections in this study.

The potential energy surface of the ESDPT in isotopically substituted 7AI–water complexes was calculated at the CASSCF(10,9)/6-31G(d,p) level followed by MRPT2 correction for dynamic correlation, which is depicted in Fig. 2A. No well for the intermediate was present on the potential energy curve of the ESDPT in the gas phase, and no intermediate was found in the aqueous phase calculations, as described earlier. The changes in O–H and N–H bond distances along the reaction coordinate were shown in Fig. 2B. As the reaction proceeded from the reactant to product, the ^{10}H atom moved rapidly at about $s = -0.7$ bohr from ^1N in the 5-membered ring to ^{16}O, followed by the ^{18}H atom moving rather slowly from ^{16}O to ^7N in the 6-membered ring. As a result, the $r(^1N–^{10}H)$ and $r(^{10}O–^{10}H)$ values crossed near the conventional TS, whereas the $r(^{16}O–^{18}H)$ and $r(^7N–^{18}H)$ values crossed at about $s = 0.5$ bohr. These results indicate that two protons were transferred very asynchronously, albeit concertedly.

The relative ZPEs (in terms of those at reactant) and vibrationally adiabatic energy curves along the MEP of the ESDPT in the isotopically substituted 7AI:H_2O complexes are depicted in Fig. 3. The zero of these adiabatic energy curves was the ZPE-corrected energies of reactant complexes. In this study, the first hydrogen or deuterium represents ^{10}H or ^{10}D, respectively, and the second hydrogen or deuterium represents ^{18}H or ^{18}D, respectively. The secondary proton (^{17}H) in H_2O was not substituted in order for the RGM not to be contaminated by the α-secondary KIE. The potential energy was decreased as the reaction proceeded from conventional TS to either product or reactant, whereas the ZPE increased rapidly. The increase in ZPE is attributed to the change in the vibrational modes involved in the protons in transfer, i.e., the stretching and bending modes of N···H···O. As the elongated N–H or O–H bonds at the TS become equilibrium bonds at reactant or product again, the stretching and bending frequencies become larger and smaller, respectively. Since the magnitude of stretching frequency is much larger than the bending frequencies, the ZPE usually increases as the reaction goes to reactant or product from TS. The decrease in the potential energy and the increase in the ZPE along the MEP are not necessarily the same, particularly when the ZPE increases faster than the potential energy decreases, therefore, the maximum in the adiabatic energy curve does not match with the maximum of the potential energy curve. This phenomena has been reported and discussed previously in the hydride transfer reaction of NAD^+ analogues in solution [60]. In addition, the asynchronicity of the double proton transfer resulted in the maximum of the adiabatic energy curve depending on the isotopic substitution.

It is interesting to note that, as shown in Fig. 3A, the minimum in the relative ZPEs is not at the conventional TS, but depends very much on the isotopic substitutions due to the asynchronicity of the ESDPT. Fig. 3B shows that the adiabatic energy curves for HH and HD, and DH and DD nearly overlapped with each other at $s < -0.3$ bohr and $s < -0.4$ bohr, respectively. These overlapped adiabatic energy curves were attributed to the nearly identical zero-point energies, which indicated that the isotopic substitution for the ^{18}H atom did not make a big change in the ZPEs when the reaction proceeded from reactant to $s = -0.3$ bohr and $s = -0.4$ bohr in the HH and HD, and DH and DD reactions, respectively, as depicted in Fig. 3A. This phenomena correlated with the $^{16}O–^{18}H$ distance along the reaction coordinate as shown in Fig. 2B, which changed very little at $s < -0.3$ bohr. Likewise, the adiabatic energy curves for the HH and DH reactions overlapped with each other at

Table 2
Selected bond lengths in Å for the reactant (normal form), product (tautomer), conventional TS, and the variational TS at 0 K in the S_1 electronic state.

	R	TS[a]	P	$^{10}H^{18}H$ (−0.79)[b]	$^{10}H^{18}D$ (−0.79)	$^{10}D^{18}H$ (−0.24)	$^{10}D^{18}D$ (−0.14)
^{1}N–^{10}H	0.999	1.258	2.190	1.033	1.034	1.187	1.216
^{16}O–^{10}H	2.136	1.220	0.949	1.564	1.560	1.297	1.266
^{7}N–^{18}H	2.126	1.444	0.996	1.590	1.570	1.497	1.467
^{16}O–^{18}H	0.952	1.086	2.196	0.987	0.993	1.042	1.066
^{8}C–^{16}O	3.340	2.797	3.443	2.826	2.822	2.800	2.799

[a] The conventional TS.
[b] The position (in bohr) of the maximum in the adiabatic energy curve, which is the variational TS at 0 K, along the mass-scaled reaction coordinate by 1 amu.

$s > 0.4$ bohr, and so were the adiabatic energy curves for the HD and DD reactions. This was attributed to the change in the ^{1}N–^{10}H distance along the reaction coordinate as shown in Fig. 2B, which was nearly completed where $s > 0.4$ bohr. Therefore, no big change in ZPEs was present due to the isotopic substitution for the ^{10}H atom as depicted in Fig. 3A. The overlapping adiabatic energy curves that appeared in the reaction coordinate of the ESDPT resulted from the ^{10}H or ^{18}H protons that act as a spectator depending on the location of the reaction coordinate. These results imply that in asynchronous double proton transfer the adiabatic energy curves are independent of the mass ratio of substituted isotopes, which result in the breakdown of the rule of the geometric mean.

The ZPE-corrected barrier heights calculated using the conventional TS of the $^{10}H^{18}H$, $^{10}H^{18}D$, $^{10}D^{18}H$, and $^{10}D^{18}D$-substituted complexes were 6.03, 6.62, 6.91, and 7.55 kcal/mol, respectively. The maximum of the vibrationally adiabatic energy curve in the S_1 state was the variational TS of the ESDPT at 0 K, which was denoted as "VTS0" in this study. It is interesting to note that no adiabatic energy curve has its maximum at $s = 0$ bohr, which means that its maximum does not appear at the conventional TS. The VTS0s for the HH, HD, DH, and DD transfer appeared at very different positions in the reaction coordinates, which were at $s = -0.79$, -0.79, -0.23, and -0.14 bohr, respectively. This phenomenon resulted from ZPE changes along the reaction coordinates of the asynchronous reactions depending on the isotopic substitution, which were termed "variational ZPE effect" in this study. The structures, energies, and frequencies at the variational TS are important to the rate calculations. Some geometric parameters at the VTS0 for HH, HD, DH, and DD transfer are listed in Table 2. The position of the variational TS was nearly independent of temperature. The geometric parameters of the VTS0 for the HH and HD reactions were nearly the same, and those for the DD reaction were very close to the conventional TS. For HH and HD reactions, the ^{1}N–^{10}H and ^{16}O–^{18}H bond distances at the VTS0 ($s = -0.79$) were very different from those of the conventional TS, but close to the reactant. For the DD reaction, these bond distances at the VTS0 ($s = -0.14$ bohr) were 0.213 and 0.112 Å larger than the corresponding reactant values, but only 0.046 and 0.022 Å smaller than those at the conventional TS, respectively. The VTS0 structures for HH and HD transfer were very similar to the reactant except that they had shorter hydrogen bonds. However the structure of the VTS0 for DD transfer was closer to the conventional TS. It is interesting to note that the VTS0 for both HH and HD reactions was located where the ^{1}N–^{10}H and ^{16}O–^{18}H bonds were about to change, or where the hydrogenic motion was about to start in the reaction coordinate. The reactive processes before the VTS0 for the HH and HD reactions were mostly heavy atom motions that brought the 7AI and H_2O molecules closer. The hydrogenic motion involving the ^{10}H atom became more important at the conventional TS.

The rate constants and tunneling coefficients calculated by variational transition state theory including multidimensional tunneling approximation are listed in Table 3 for the HH, HD, DH, and DD transfers. The k^{CVT} values for the HH transfer were about 4–8 times smaller than the k^{TST} values, which were calculated by conventional transition state theory (TST), due to the large variational effect depending on the temperature. The differences between CVT and TST rate constants in the DD transfers were not large because the variational TS was not very different from the conventional TS, as shown in Fig. 3B. The variational effect of rate constants in HD transfer was larger than in DH transfer, which was consistent with the relative positions of the variational TS in these reactions as shown in Fig. 3B. The SCT tunneling coefficients of the HD reactions were larger than those of the DH reactions. However, in general, the tunneling coefficients were fairly small as a consequence of the flat adiabatic energy curves of the ESDPT.

Table 3
Rate constants (s^{-1}) and tunneling coefficients calculated by conventional and variational transition state theory with and without the SCT approximation for HH, HD, DH, and DD reactions.

T (K)	k^{TST}	k^{CVT}	$k^{CVT/SCT}$	κ^{SCT}
$^{10}H^{18}H$				
250	1.45×10^{6}	1.89×10^{5}	5.63×10^{5}	2.99
298	9.98×10^{6}	1.91×10^{6}	4.14×10^{6}	2.20
300	1.07×10^{7}	2.07×10^{6}	4.44×10^{6}	2.17
311	1.51×10^{7}	3.14×10^{6}	6.41×10^{6}	2.07
350	4.29×10^{7}	1.10×10^{7}	1.95×10^{7}	1.79
$^{10}H^{18}D$				
250	4.65×10^{5}	1.77×10^{5}	4.08×10^{5}	2.30
298	3.71×10^{6}	1.86×10^{6}	3.27×10^{6}	1.83
300	3.98×10^{6}	2.01×10^{6}	3.49×10^{6}	1.81
311	5.79×10^{6}	3.06×10^{6}	4.99×10^{6}	1.74
350	1.79×10^{7}	1.07×10^{7}	1.57×10^{7}	1.56
$^{10}D^{18}H$				
250	1.93×10^{5}	1.16×10^{5}	2.10×10^{5}	1.80
298	1.78×10^{6}	1.15×10^{6}	1.74×10^{6}	1.51
300	1.92×10^{6}	1.25×10^{6}	1.87×10^{6}	1.50
311	2.87×10^{6}	1.89×10^{6}	2.74×10^{6}	1.46
350	9.61×10^{6}	6.57×10^{6}	8.80×10^{6}	1.34
$^{10}D^{18}D$				
250	8.06×10^{4}	7.51×10^{4}	1.22×10^{5}	1.63
298	8.37×10^{5}	7.85×10^{5}	1.10×10^{6}	1.41
300	9.07×10^{5}	8.51×10^{5}	1.19×10^{6}	1.40
311	1.38×10^{6}	1.30×10^{6}	1.77×10^{6}	1.37
350	4.95×10^{6}	4.66×10^{6}	5.95×10^{6}	1.28

The variational effect depending on isotopes resulted in a significant change in the KIE, where the KIEs calculated with CVT rate constants became very different from those using TST rate constants. The calculated KIEs at 298 K are listed in Table 4. The conventional TST and CVT without tunneling correction predicted

Table 4
Kinetic isotope effects at 298 K calculated by conventional and variational transition state theory with and without the SCT approximation for HH, HD, DH, and DD reactions.

	TST	CVT	CVT/SCT	SCT
$^{10}H^{18}H/^{10}H^{18}D$	2.69	1.03	1.27	1.20
$^{10}H^{18}H/^{10}D^{18}H$	5.59	1.66	2.39	1.46
$^{10}H^{18}D/^{10}D^{18}D$	4.43	2.36	2.97	1.30
$^{10}D^{18}H/^{10}D^{18}D$	2.13	1.47	1.58	1.07
$^{10}H^{18}H/^{10}D^{18}D$	11.9	2.43	3.76	1.56

the HH/DD KIEs of 11.9 and 2.43, respectively. The tunneling contribution to the HH/DD KIE, which is the ratio of transmission coefficients, was 1.6. Compared with experimental HH/DD KIEs measured in aqueous solution, which were 3.4 [20] at 297 K and 3.7 [10] at 293 K, the KIEs from the TST were too big, whereas those from the CVT were too small. However, the HH/DD KIE obtained from CVT including the SCT approximation was 3.76, which agreed remarkably well with the experiments in water. No special approximations were made to reproduce the experimental KIEs in aqueous solution in this study.

4. Discussion

The tautomerization of 7AI in condensed phase was observed experimentally [10,20,21]. Chapman and Maroncelli [20] reported that the rate constants varied from $10^9\ s^{-1}$ in room temperature for the tautomerization of 7AI in water. The breakdown of the RGM was observed in water suggesting the stepwise ESDPT mechanism [10], and the observed HH/DD KIEs were in the range of 3.4–3.9 at room temperature [10,20,25]. To apply transition state theory in excited state reactions, the excited species should be thermally equilibrated with environment during the reactive processes. In solution, this equilibrium is reached by solvent relaxation. If the solvent relaxation is slower than the reactive process so that the equilibrium condition cannot be maintained, transition state theory may not be applied. Jimenez et al. [61] measured ultrafast solvation dynamics of water, which is faster than 50 fs, using a coumarin probe. Furthermore, the temperature dependence of the ESDPT rate was measured, and linear Arrhenius plots of $\ln k_{PT}$ vs. $1/T$ were observed both in water and in methyl alcohol [20,24]. These results mean that the solvent relaxation in water is much faster than the excited state tautomerization reaction, and confirm that transition state theory can be used to study the ESDPT in water. In addition, the vibrational modes orthogonal to the reaction coordinate are less sensitive to the solvent effect, and so are the KIEs. The environmental effects are cancelled out to some extent when we take ratio of the rate constants for the KIE. Therefore appropriate prediction of KIE based on the gas phase reaction dynamics calculations could provide a reasonable insight for the condensed phase reaction dynamics unless the overall mechanism is changed greatly due to the solvent effect. This and previous studies [34] showed that the overall mechanism of ESDPT in water would be the same as that in the gas phase.

Comparing to experimental results in water, the rate constants in this study were about a few hundred times smaller. The IEFPCM model calculations and the use of slightly larger basis sets in this study reduced the conventional barrier height by about 2.7 kcal/mol, which would increase rate constants by a factor of 96 at 298 K. If we recalculate the CVT/SCT rate constants using this factor, although it is a very crude approximation, our rate constants are in the order of 10^8, which agree well with experimental values [10,20]. Although the calculated KIEs were based on the gas phase reaction coordinates, it would be impossible to obtain good agreement if the reaction mechanisms were significantly different with each other. Both variational and tunneling effects would be essential to reproduce the experimental values. If one of them is missing or incorrectly considered, experimental KIEs are hardly reproduced within reasonable amount of error.

7AI has two protons, ^{10}H and ^{18}H, that can be substituted by deuterium. In general, the RGM in the KIEs should be satisfied in the concerted double proton transfer reactions. Table 4 shows that the KIEs for mono-substituted complexes depended very much on the substituted position. The KIE values calculated by the conventional TST were always larger than those using CVT, which was attributed to the variational ZPE effect that reduced the energy difference of variational TS between isotopically substituted reactions. For example, the HH/HD KIE using the CVT was only 1.03, which was due to the very small energy difference between variational TSs for the HH and HD reactions as shown in Fig. 3B. However, this difference between saddle points was much larger, which resulted in larger HH/HD KIE using the TST values compared to those using CVT. The difference of adiabatic energy barriers between HH, HD, DH, and DD reactions were reduced significantly due to the variational ZPE effect. The adiabatic energy barriers for HH, HD, DH, and DD reactions were 7.56, 7.64, 7.63, and 7.83 kcal/mol, respectively, and the largest difference was only 0.27 kcal/mol between the HH and DD reactions. Without considering the variational ZPE effect, this difference would be 1.52 kcal/mol, which was obtained using the conventional TS. Because the adiabatic energy barrier of the HH transfer was increased more than that of the DD transfer due to the variational ZPE effect, the difference between CVT and TST rate constants were very large for the HH transfer, but small for the DD transfer.

The substitution for ^{10}H generated larger KIEs than ^{18}H, which was attributed to the hydrogenic motions of these protons at their conventional or variational TSs, where ^{10}H always moved earlier than ^{18}H, which led to larger frequency change with the ^{10}H substitution. The asynchronicity in the hydrogenic motion of these two protons breaks the underlying assumption of the RGM that changes in the force constants of isotopically sensitive bonds at the transition state that are broken or formed during the concerted reaction are approximately the same. When this assumption is broken, the $k_{HH}/k_{HD} \approx k_{HD}/k_{DD}$ relation is no longer valid, although the secondary KIE is negligible. Table 4 clearly shows that the HH/HD KIEs without tunneling were already very different from the HD/DD KIEs, which indicates the breakdown of the RGM. In addition, the secondary KIE was not negligible. In the HH/HD and DH/DD KIEs where ^{10}H was the secondary proton, the secondary KIEs were 1.43 and 0.79, using CVT and TST, respectively. The secondary KIEs with ^{18}H as a secondary proton were the same as these values. These values are not small as a secondary KIE in general. It is interesting to note that the inverse secondary isotope effects using TST became normal when using CVT. This significant change originated from the variational ZPE effect depending on the substituted complexes that were used for the rate calculations. This study clearly showed that the variational ZPE effect originated from the asynchronicity of the ESDPT breaks the RGM, which has been used for many years as an experimental criterion for the concerted mechanism. The asynchronicity of the ESDPT became more significant in aqueous solution, therefore the solvent effect would not alter the conclusion of this study.

5. Conclusions

We have presented a direct *ab initio* reaction dynamics study for the excited state tautomerization of a 1:1 7AI:H_2O complex with isotopic substitutions using variational transition state theory including multidimensional tunneling approximation. The potential energy surfaces were generated at the MRPT2//CASSCF(10,9) level using the IVTST-M algorithm with the interpolated single point energy correction. The rate constants and KIEs were calculated to test the RGM, which has been used for many years as a criterion for the concerted double proton transfer reactions. This study shows that the ESDPT in 1:1 7AI:H_2O complexes occurs via a concerted albeit asynchronous mechanism. The vibrationally adiabatic energy surfaces in the S_1 electronic state depended on isotopes, which resulted in a large variational effect even at 0 K.

The asynchronicity of two protons in flight breaks the underlying assumption of the RGM, i.e., the changes in the force constants of isotopically sensitive bonds at the transition state that are broken or

formed during the concerted reaction are approximately the same. Because this assumption is broken, the relation, $k_{HH}/k_{HD} \approx k_{HD}/k_{DD}$, is no longer valid in asynchronous double proton transfer, although the secondary KIE is negligible. This study shows that the RGM breaks down in the ESDPT in 1:1 7AI:H_2O complexes due to the asynchronous processes. Therefore the breakdown of the RGM should not be used as absolute evidence for the stepwise mechanism.

Acknowledgments

This research was supported in part by Basic Science Research Program through the National Research Foundation of Korea (NRF) funded by the Ministry of Education, Science and Technology (grant number 2010-0012990). My Phu Thi Doung acknowledges financial support from the Korean Research Foundation.

References

[1] M.L. Bender, Mechanisms of Homogeneous Catalysis from Protons to Proteins, John Wiley & Sons, New York, 1971.
[2] L. Melander, W.H. Saunders Jr., Reaction Rates of Isotopic Molecules, John Wiley & Sons, New York, 1980.
[3] J. Braun, H.-H. Limbach, P.G. Williams, H. Morimoto, D.E. Wemmer, Observation of kinetic tritium isotope effects by dynamic NMR. The tautomerism of porphyrin, J. Am. Chem. Soc. 118 (1996) 7231–7232.
[4] H.H. Limbach, Single and multiple hydrogen/deuterium transfer reactions in liquids and solids, in: R.L. Schowen, J.P. Klinman, J.T. Hynes, H.H. Limbach (Eds.), Hydrogen-Transfer Reactions, Wiley-VCH, Weinheim, 2007.
[5] D. Gerritzen, H.-H. Limbach, Kinetic isotope effects and tunneling in cyclic double and triple proton transfer between acetic acid and methanol in tetrahydrofuran studied by dynamic proton and deuteron NMR spectroscopy, J. Am. Chem. Soc. 106 (1984) 869–879.
[6] G. Scherer, H.-H. Limbach, Observation of a stepwise double proton transfer in oxalamidine which involves matched kinetic hydrogen–hydrogen/hydrogen–deuterium/deuterium–deuterium isotope and solvent effects, J. Am. Chem. Soc. 111 (1989) 5946–5947.
[7] M. Schlabach, H.-H. Limbach, A. Shu, E. Bunnenberg, B. Tolf, C. Djerassi, NMR study of kinetic HH/HD/DH/DD isotope effects on the tautomerism of acetylporphyrin: evidence for a stepwise double proton transfer, J. Am. Chem. Soc. 115 (1993) 4554–4565.
[8] C.A. Tayler, M.A. El-Bayoumi, M. Kasha, Excited-state two-proton tautomerism in hydrogen-bonded N-heterocyclic base pairs, Proc. Natl. Acad. Sci. U.S.A. 63 (1969) 253–260.
[9] J. Catalan, J.C. del Valle, M. Kasha, Resolution of concerted versus sequential mechanisms in photo-induced double-proton transfer reaction in 7-azaindole H-bonded dimer, Proc. Natl. Acad. Sci. U.S.A. 96 (1999) 8338–8343.
[10] Y. Chen, F. Gai, J.W. Petrich, Solvation of 7-azaindole in alcohols and water: evidence for concerted, excited-state, double-proton transfer in alcohols, J. Am. Chem. Soc. 115 (1993) 10158–10166.
[11] P.T. Chou, W.S. Yu, C.Y. Wei, Y.M. Cheng, C.Y. Yang, Water-catalyzed excited-state double proton transfer in 3-cyano-7-azaindole: the resolution of the proton-transfer mechanism for 7-azaindoles in pure water, J. Am. Chem. Soc. 123 (2001) 3599–3600.
[12] A. Douhal, S.K. Kim, A.H. Zewail, Femtosecond molecular dynamics of tautomerization in model base pairs, Nuture 378 (1995) 260–263.
[13] D.E. Folmer, E.S. Wisniewski, J.R. Stairs, J.A.W. Castleman, Water-assited proton transfer in the monomer of 7-azaindole, J. Phys. Chem. A 104 (2000) 10545–10549.
[14] A. Hara, K. Sakota, M. Nakagaki, H. Sekiya, Dispersed fluorescence spectra of jet-cooled 7-azaindole-$(H_2O)_n$ (n = 1–3): does photoinduced excited-state proton transfer occur or not? Chem. Phys. Lett. 407 (2005) 30–34.
[15] S. Takeuchi, T. Tahara, The answer to concerted versus step-wise controversy for the double proton transfer mechanism of 7-azaindole dimer in solution, Proc. Natl. Acad. Sci. U.S.A. 104 (2007) 5285–5290.
[16] O.H. Kwon, A.H. Zewail, Double proton transfer dynamics of model DNA base pairs in the condensed phase, Proc. Natl. Acad. Sci. U.S.A. 104 (2007) 8703–8708.
[17] H. Sekiya, K. Sakota, Excited-state double-proton transfer in the 7-azaindole dimer in the gas phase. resolution of the stepwise versus concerted mechanism controversy and a new paradigm, Bull. Chem. Soc. Jpn. 79 (2006) 373–385.
[18] G.M. Chaban, M.S. Gordon, The ground and excited state hydrogen transfer potential energy surface in 7-azaindole, J. Phys. Chem. A 103 (1999) 185–189.
[19] M.S. Gordon, Hydrogen transfer in 7-azaindole, J. Phys. Chem. 100 (1996) 3974–3979.
[20] C.F. Chapman, M. Maroncelli, Excited-state tautomerlzation of 7-azaindoie in water, J. Phys. Chem. 96 (1992) 8430–8441.
[21] P.-T. Chou, M.L. Martinez, W.C. Cooper, D. McMorrow, S.T. Collins, M. Kasha, Monohydrate catalysis of excited-state double-proton transfer in 7-azaindole, J. Phys. Chem. 96 (1992) 5203–5205.
[22] O.-H. Kwon, Y.-S. Lee, H.J. Park, Y. Kim, D.-J. Jang, Asymmetric double proton transfer of excited 1:1 7-azaindole/alcohol complexes with anomalously large and temperature-independent kinetic isotope effects, Angew. Chem. 43 (2004) 5792–5796.
[23] S. Mente, M. Maroncelli, Solvation and the excited-state tautomerization of 7-azaindole and 1-azacarbazole: computer simulations in water and alcohol solvents, J. Phys. Chem. A 102 (1998) 3860–3876.
[24] R.S. Moog, M. Maroncelli, 7-Azaindole in alcohols: solvation dynamics and proton transfer, J. Phys. Chem. 95 (1991) 10359–10369.
[25] P.-T. Chou, W.-S. Yu, C.-Y. Wei, Y.-M. Cheng, C.-Y. Yang, Water-catalyzed excited-state double proton transfer in 3-cyano-7-azaindole: the resolution of the proton-transfer mechanism for 7-azaindoles in pure water, J. Am. Chem. Soc. 123 (2001) 3599–3600.
[26] W.-T. Hsieh, C.-C. Hsieh, C.-H. Lai, Y.-M. Cheng, M.-L. Ho, K.K. Wang, G.-H. Lee, P.-T. Chou, Excited-state double proton transfer in model base pairs: the stepwise reaction on the heterodimer of 7-azaindole analogues, ChemPhysChem 9 (2008) 293–299.
[27] K.S. Venkatasubban, R.L. Schowen, The proton inventory technique, CRC Crit. Rev. Biochem. 17 (1984) 1–44.
[28] J. Bigeleisen, Statistical mechanics of isotopic systems with small quantum corrections. I. General considerations and the rule of the geometric mean, J. Chem. Phys. 23 (1955) 2264–2267.
[29] L. Meschede, H.-H. Limbach, Dynamic NMR study of the kinetic HH/HD/DD isotope effects on the double proton transfer in cyclic bis(p-fluorophenyl)formamidine dimers, J. Phys. Chem. 95 (1991) 10267–10280.
[30] H. Rumpel, H.-H. Limbach, NMR study of kinetic HH/HD/DD isotope, solvent and solid-state effects on the double proton transfer in azophenine, J. Am. Chem. Soc. 111 (1989) 5429–5441.
[31] H.H. Limbach, J. Hennig, D.G. Gerritzen, H. Rumpel, Primary kinetic HH/HD/DH/DD isotope effects and proton tunnelling in double proton-transfer reactions, Faraday Dis. Chem. Soc. 74 (1982) 229–243.
[32] M. Amin, R.C. Price, W.H.J. Saunders, Isotope effects on isotope effects. Failure of the rule of the geometric mean as evidence for tunneling, J. Am. Chem. Soc. 110 (1988) 4085–4586.
[33] R.L. Bell, T.N. Truong, Primary and solvent kinetic isotope effects in the water-assisted tautomerization of formamidine: an ab initio direct dynamics study, J. Phys. Chem. A 101 (1997) 7802–7808.
[34] D. Kina, A. Nakayama, T. Noro, T. Taketsugu, M.S. Gordon, Ab initio QM/MM molecular dynamics study on the excited-state hydrogen transfer of 7-azaindole in water solution, J. Phys. Chem. A 112 (2008) 9675–9683.
[35] J.-H. Lim, E.K. Lee, Y. Kim, Theoretical study for solvent effect on the potential energy surface for the double proton transfer in formic acid dimer and formamidine dimer, J. Phys. Chem. A 101 (1997) 2233–2239.
[36] F.-T. Hung, W.-P. Hu, T.-H. Li, C.-C. Cheng, P.-T. Chou, Ground and excited-state acetic acid catalyzed double proton transfer in 2-aminopyridine, J. Phys. Chem. A 107 (2003) 3244–3253.
[37] A. Kyrychenko, J. Waluk, Excited-state proton transfer through water bridges and structure of hydrogen-bonded complexes in 1H-pyrrolo[3,2-h]quinoline: adiabatic time-dependent density functional theory study, J. Phys. Chem. A 110 (2006) 11958–11967.
[38] K. Nam, Y. Kim, Direct ab initio dynamics calculations for rates and the kinetic isotope effects of multiproton transfer in $ClONO_2 + HCl \rightarrow HNO_3 + Cl_2$ reactions with water clusters: breakdown of the rule of the geometric mean, J. Chem. Phys. 130 (2009) 144310–144320.
[39] Y. Podolyan, L. Gorb, J. Leszczynski, Double-proton transfer in the formamidine–formamide dimer. Post-hartree-fock gas-phase and aqueous solution study, J. Phys. Chem. A 106 (2002) 12103–12109.
[40] Y. Kim, S. Lim, Y. Kim, The role of a short and strong hydrogen bond on the double proton transfer in the formamidine–formic acid complex: theoretical studies in the gas phase and in solution, J. Phys. Chem. A 103 (1999) 6632–6637.
[41] J.C. Corchado, E.L. Coitiño, Y.-Y. Chuang, P.L. Fast, D.G. Truhlar, Interpolated variational transition-state theory by mapping, J. Phys. Chem. A 102 (1998) 2424–2438.
[42] M.J. Frisch, G.W. Trucks, H.B. Schlegel, G.E. Scuseria, M.A. Robb, J.R. Cheeseman, J.A. Montgomery Jr., T. Vreven, K.N. Kudin, J.C. Burant, J.M. Millam, S.S. Iyengar, J. Tomasi, V. Barone, B. Mennucci, M. Cossi, G. Scalmani, N. Rega, G.A. Petersson, H. Nakatsuji, M. Hada, M. Ehara, K. Toyota, R. Fukuda, J. Hasegawa, M. Ishida, T. Nakajima, Y. Honda, O. Kitao, H. Nakai, M. Klene, X. Li, J.E. Knox, H.P. Hratchian, J.B. Cross, V. Bakken, C. Adamo, J. Jaramillo, R. Gomperts, R.E. Stratmann, O. Yazyev, A.J. Austin, R. Cammi, C. Pomelli, J.W. Ochterski, P.Y. Ayala, K. Morokuma, G.A. Voth, P. Salvador, J.J. Dannenberg, V.G. Zakrzewski, S. Dapprich, A.D. Daniels, M.C. Strain, O. Farkas, D.K. Malick, A.D. Rabuck, K. Raghavachari, J.B. Foresman, J.V. Ortiz, Q. Cui, A.G. Baboul, S. Clifford, J. Cioslowski, B.B. Stefanov, G. Liu, A. Liashenko, P. Piskorz, I. Komaromi, R.L. Martin, D.J. Fox, T. Keith, M.A. Al-Laham, C.Y. Peng, A. Nanayakkara, M. Challacombe, P.M.W. Gill, B. Johnson, W. Chen, M.W. Wong, C. Gonzalez, J.A. Pople, Gaussian 03, Gaussian, Inc., Wallingford, CT, 2004.
[43] K. Hirao, Multireference Møller–Plesset method, Chem. Phys. Lett. 190 (1992) 374–380.
[44] K. Hirao, Multireference Møller–Plesset perturbation theory for high-spin open-shell systems, Chem. Phys. Lett. 196 (1992) 397–403.
[45] K. Hirao, State-specific multireference Møller–Plesset perturbation treatment for singlet and triplet excited states, ionized states and electron attached states of H_2O, Chem. Phys. Lett. 201 (1993) 59–66.

[46] M.T. Cancès, B. Mennucci, J. Tomasi, New integral equation formalism for the polarizable continuum model: theoretical background and applications to isotropic and anisotropic dielectrics, J. Chem. Phys. 107 (1997).
[47] M. Cossi, V. Barone, B. Mennucci, J. Tomasi, Ab initio study of ionic solutions by a polarizable continuum dielectric model, Chem. Phys. Lett. 286 (1998) 253–260.
[48] B. Mennucci, J. Tomasi, Continuum solvation models: a new approach to the problem of solute's charge distribution and cavity boundaries, J. Chem. Phys. 106 (1997) 5151–5158.
[49] M.J. Frisch, G.W. Trucks, H.B. Schlegel, G.E. Scuseria, M.A. Robb, J.R. Cheeseman, G. Scalmani, V. Barone, B. Mennucci, G.A. Petersson, H. Nakatsuji, M. Caricato, X. Li, H.P. Hratchian, A.F. Izmaylov, J. Bloino, G. Zheng, J.L. Sonnenberg, M. Hada, M. Ehara, K. Toyota, R. Fukuda, J. Hasegawa, M. Ishida, T. Nakajima, Y. Honda, O. Kitao, H. Nakai, T. Vreven, J.A. Montgomery Jr., J.E. Peralta, F. Ogliaro, M. Bearpark, J.J. Heyd, E. Brothers, K.N. Kudin, V.N. Staroverov, R. Kobayashi, J. Normand, K. Raghavachari, A. Rendell, J.C. Burant, S.S. Iyengar, J. Tomasi, M. Cossi, N. Rega, J.M. Millam, M. Klene, J.E. Knox, J.B. Cross, V. Bakken, C. Adamo, J. Jaramillo, R. Gomperts, R.E. Stratmann, O. Yazyev, A.J. Austin, R. Cammi, C. Pomelli, J.W. Ochterski, R.L. Martin, K. Morokuma, V.G. Zakrzewski, G.A. Voth, P. Salvador, J.J. Dannenberg, S. Dapprich, A.D. Daniels, O. Farkas, J.B. Foresman, J.V. Ortiz, J. Cioslowski, D.J. Fox, Gaussian 09, Gaussian, Inc., Wallingford, CT, 2009.
[50] Y.-Y. Chuang, J.C. Corchado, D.G. Truhlar, Mapped interpolation scheme for single-point energy corrections in reaction rate calculations and a critical evaluation of dual-level reaction-path dynamics methods, J. Phys. Chem. A 103 (1999) 1140–1149.
[51] M.W. Schmidt, K.K. Baldridge, J.A. Boatz, S.T. Elbert, M.S. Gordon, J.H. Jensen, S. Koseki, N. Matsunaga, K.A. Nguyen, S.J. Su, T.L. Windus, M. Dupuis, J.A. Montgomery, General atomic and molecular electronic structure system, J. Comput. Chem. 14 (1993) 1347–1363.
[52] Y.-P. Liu, G.C. Lynch, T.N. Truong, D.-H. Lu, D.G. Truhlar, B.C. Garrett, Molecular modeling of the kinetic isotope effect for the [1,5]-sigmatropic rearrangement of cis-1,3-pentadiene, J. Am. Chem. Soc. 115 (1993) 2408–2415.
[53] R.T. Skodje, D.G. Truhlar, B.C. Garrett, A general small-curvature approximation for transition-state-theory transmission coefficients, J. Phys. Chem. 85 (1981) 3019–3023.
[54] D.G. Truhlar, A.D. Isaacson, B.C. Garrett, in: M. Baer (Ed.), Theory of Chemical Reaction Dynamics, CRC Press, Boca Raton, FL, 1985, p. 65.
[55] A. Fernández-Ramos, B.A. Ellingson, B.C. Garrett, D.G. Truhlar, in: K.B. Lipkowitz, T.R. Cundari (Eds.), Reviews in Computational Chemistry, Wiley-VCH, Hoboken, NJ, 2007, pp. 125–232.
[56] K.K. Baldridge, M.S. Gordon, R. Steckler, D.G. Truhlar, Ab initio reaction paths and direct dynamics calculations, J. Phys. Chem. 93 (1989) 5107–5119.
[57] D.G. Truhlar, Direct dynamics method for the calculation of reaction rates, in: D. Heidrich (Ed.), The Reaction Path in Chemistry: Current Approaches and Perspectives, Kluwer, Dordrecht, The Netherlands, 1995, p. 229.
[58] J.C. Corchado, Y.-Y. Chuang, E.L. Coitiño, B.A. Ellingson, J. Zheng, D.G. Truhlar, Gaussrate-Version 9.7, University of Minnesota, Minneapolis, MN, 2007.
[59] J.C. Corchado, Y.-Y. Chuang, P.L. Fast, W.-P. Hu, Y.-P. Liu, G.C. Lynch, K.A. Nguyen, C.F. Jackels, A.F. Ramos, B.A. Ellingson, B.J. Lynch, J. Zheng, V.S. Melissas, J. Villa, I. Rossi, E.L. Coitino, J. Pu, T.V. Albu, R. Steckler, B.C. Garrett, A.D. Isaacson, D.G. Truhlar, Polyrate-Version 9.7, University of Minnesota, Minneapolis, USA, 2007.
[60] Y. Kim, M.M. Kreevoy, The experimental manifestations of corner-cutting tunneling, J. Am. Chem. Soc. 114 (1992) 7116–7123.
[61] R. Jimenez, G.R. Fleming, P.V. Kumar, M. Maroncelli, Femtosecond solvation dynamics of water, Nature 369 (1994) 471–473.